

## Supplementary Information

### Triple-Cation Low-Bandgap Perovskite Thin-Films for High-Efficiency Four-Terminal All-Perovskite Tandem Solar Cells

Somayeh Moghadamzadeh,<sup>a,b,\*</sup> Ihtez M. Hossain,<sup>b,a</sup> The Duong,<sup>c</sup> Saba Gharibzadeh,<sup>b,a</sup> Tobias Abzieher,<sup>a,b</sup> Huyen Pham,<sup>d</sup> Hang Hu,<sup>b,a</sup> Paul Fassel,<sup>b,a</sup> Uli Lemmer,<sup>a,b</sup> Bahram Abdollahi Nejad,<sup>b,a,\*</sup> and Ulrich W. Paetzold<sup>b,a,\*</sup>

<sup>a</sup> Light Technology Institute (LTI), Karlsruhe Institute of Technology (KIT), Engesserstrasse 13, 76131, Karlsruhe, Germany

<sup>b</sup> Institute of Microstructure Technology (IMT), Karlsruhe Institute of Technology (KIT), Hermann-von-Helmholtz-Platz 1, 76344 Eggenstein-Leopoldshafen, Karlsruhe, Germany

<sup>c</sup> Research School of Electrical, Energy and Materials Engineering, The Australian National University, Canberra 2601, Australia

<sup>d</sup> Department of Electronic Materials Engineering, Research School of Physics, The Australian National University, Canberra 2601, Australia

\* To whom correspondence should be addressed email: [somayeh.moghadamzadeh@kit.edu](mailto:somayeh.moghadamzadeh@kit.edu), [bahram.abdollahi@kit.edu](mailto:bahram.abdollahi@kit.edu), [ulrich.paetzold@kit.edu](mailto:ulrich.paetzold@kit.edu)

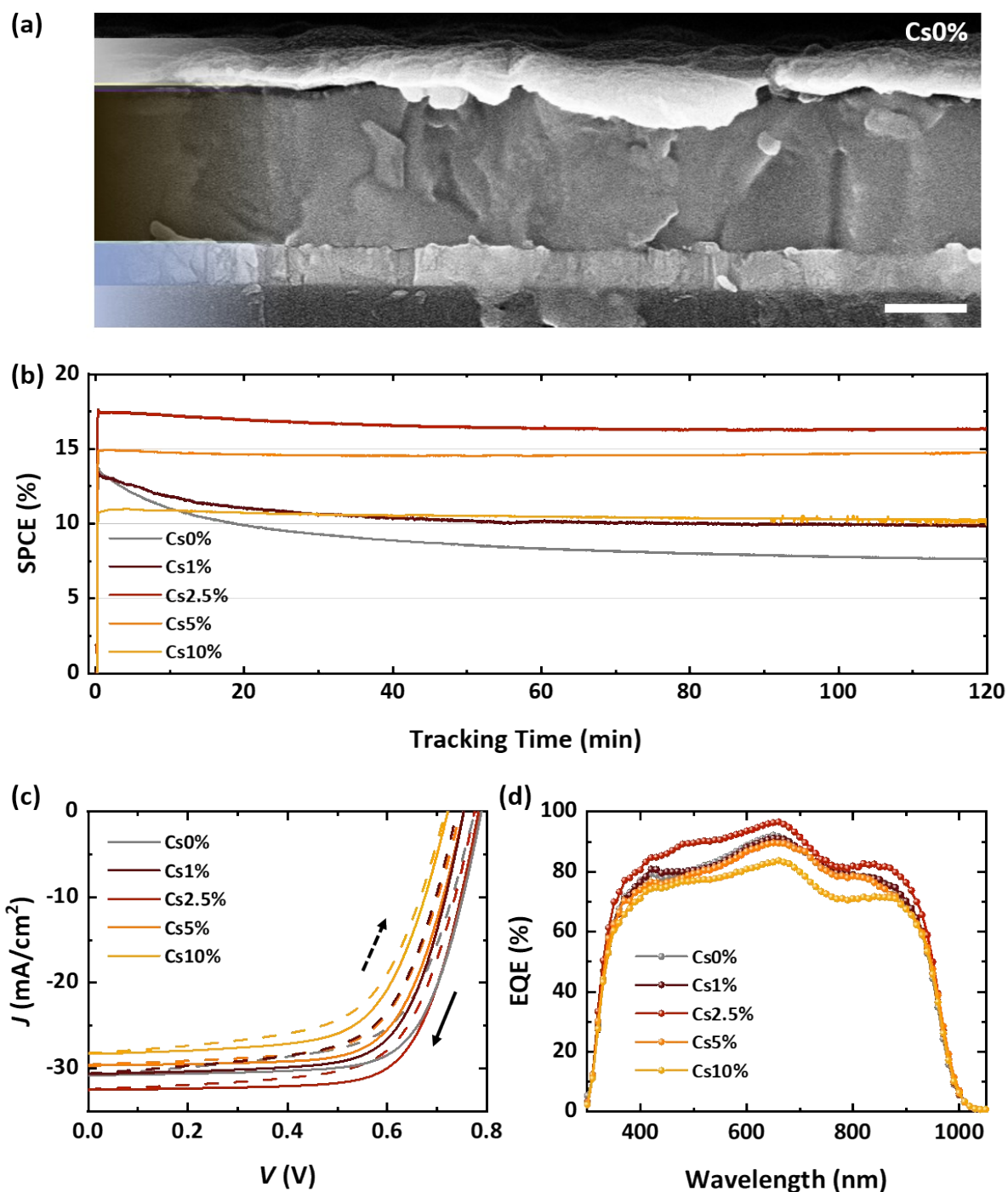


**Fig. S1.** (a) Cross-sectional SEM image of a PSC with a layer stack of glass / ITO / PTAA /  $\text{Cs}_x(\text{FA}_{0.8}\text{MA}_{0.2})_{1-x}\text{Sn}_{0.5}\text{Pb}_{0.5}\text{I}_3$  / PCBM /  $\text{C}_{60}$  / BCP / Ag, for which  $x = 0$  (denoted as Cs0%). The scalebar on the bottom-right is indicative of 300 nm. (b) Absolute values of stabilized power conversion efficiency (SPCE) at the MPP tracking conditions for 120 min, (c) current-density–voltage ( $J$ - $V$ ) scans measured at a fixed rate of 0.6 V/s from the open-circuit voltage ( $V_{\text{OC}}$ ) to the short-circuit current ( $J_{\text{SC}}$ ) (solid lines) and from  $J_{\text{SC}}$  to  $V_{\text{OC}}$  (dashed lines) under AM 1.5G illumination (100 mW/cm<sup>2</sup>) at 25°C, of the best performing LBG PSCs prepared with different Cs concentrations varying from 0% to 10% (denoted as Cs0% to Cs10%). Comparing figure a with b demonstrates that the actual PCEs of the PSCs lie in the middle between the forward and backward scans. (d) the external quantum efficiency (EQE) of devices with perovskite thin-films prepared with different Cs concentrations.

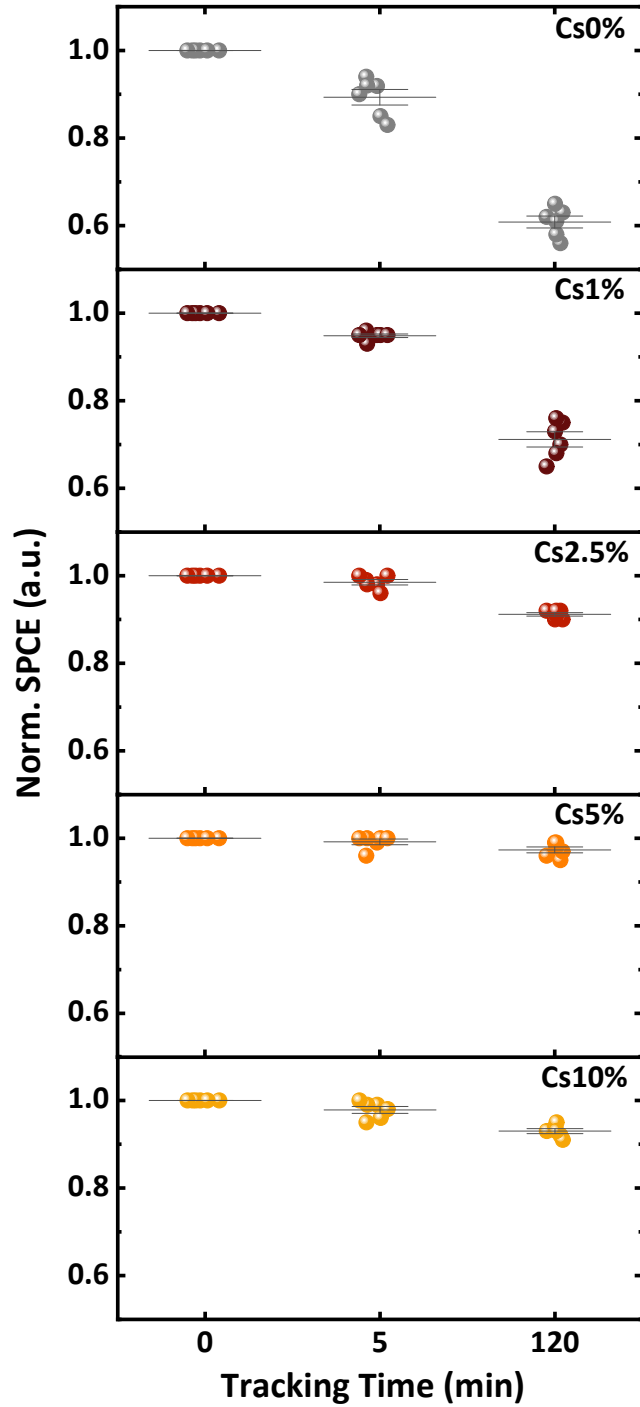


**Fig. S2.** Stabilized power conversion efficiency (SPCE) at 0 min (when the lamp is switched on), and after 5 and 120 min of maximum power point (MPP) tracking, derived from six low-bandgap perovskite solar cells (LBG PSCs) with different Cs concentrations varying from 0% (top) to 10% (bottom) which were identically-prepared in different batches. The initial values (at 0 min) are normalized to 1.

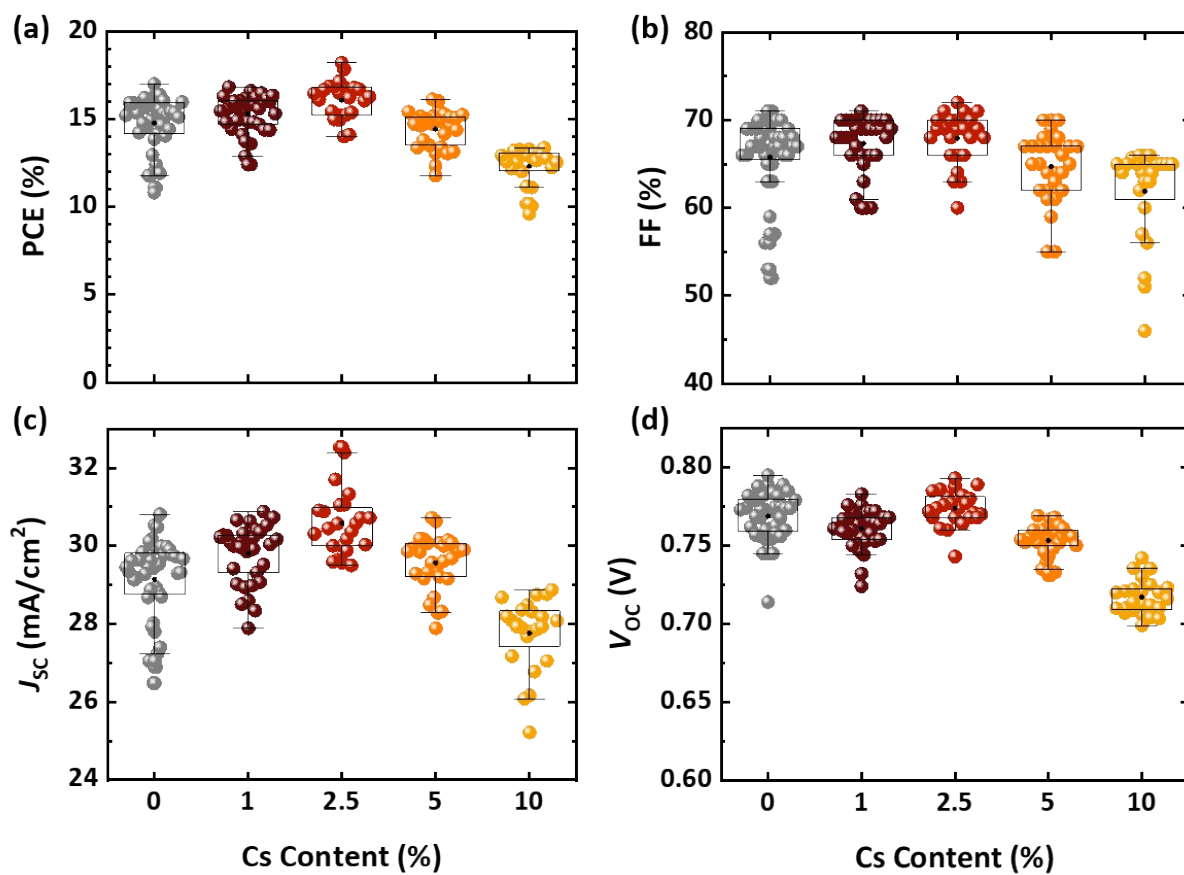


**Fig. S3.** (a) Power conversion efficiency (PCE), (b) fill factor (FF), (c) short-circuit current ( $J_{sc}$ ), and (d) open-circuit voltage ( $V_{oc}$ ) of 30 low-bandgap perovskite solar cells (LBG PSCs) with different Cs concentrations varying from 0% to 10%, identically-prepared in 10 different batches. The black dots show the average values.

**Table S1.** Photovoltaic parameters (champion (Ch.) and average (Ave.) values) of low-bandgap perovskite solar cells (LBG PSCs) with different Cs concentrations varying from 0% to 10%, derived from current-density–voltage ( $J$ – $V$ ) scans measured at a fixed rate of 0.6 V/s from the open-circuit voltage ( $V_{OC}$ ) to the short-circuit current ( $J_{SC}$ ) (backward scan) and from  $J_{SC}$  to  $V_{OC}$  (forward scan) under AM 1.5G illumination (100 mW/cm<sup>2</sup>) at 25°C. The average (Ave.) values are derived from 30 LBG PSCs identically-prepared in 10 different batches.

Cs concentration	Scan direction	$V_{OC}$ (V)		$J_{SC}$ (mA/cm <sup>2</sup> )		FF (%)		PCE (%)	
		Ch.	Ave.	Ch.	Ave.	Ch.	Ave.	Ch.	Ave.
Cs0%	Backward	0.79	0.77	30.8	29.1	70.6	65.8	17.2	14.8
	Forward	0.77	0.76	30.9	28.9	63.3	60.5	15.2	13.2
Cs1%	Backward	0.75	0.76	30.7	29.8	69.2	67.3	16.0	15.3
	Forward	0.74	0.75	30.6	29.7	63.4	62.0	14.3	13.8
Cs2.5%	Backward	0.78	0.78	32.5	30.6	71.8	68	18.2	16.1
	Forward	0.77	0.77	32.5	30.4	66.5	63.7	16.7	14.8
Cs5%	Backward	0.75	0.75	29.7	29.6	68.9	64.7	15.4	14.4
	Forward	0.75	0.75	29.6	29.3	65.7	61.2	14.5	13.3
Cs10%	Backward	0.72	0.72	28.3	27.8	65.3	62.0	13.3	12.3
	Forward	0.72	0.73	28.3	26.5	61.4	61.1	12.4	11.9

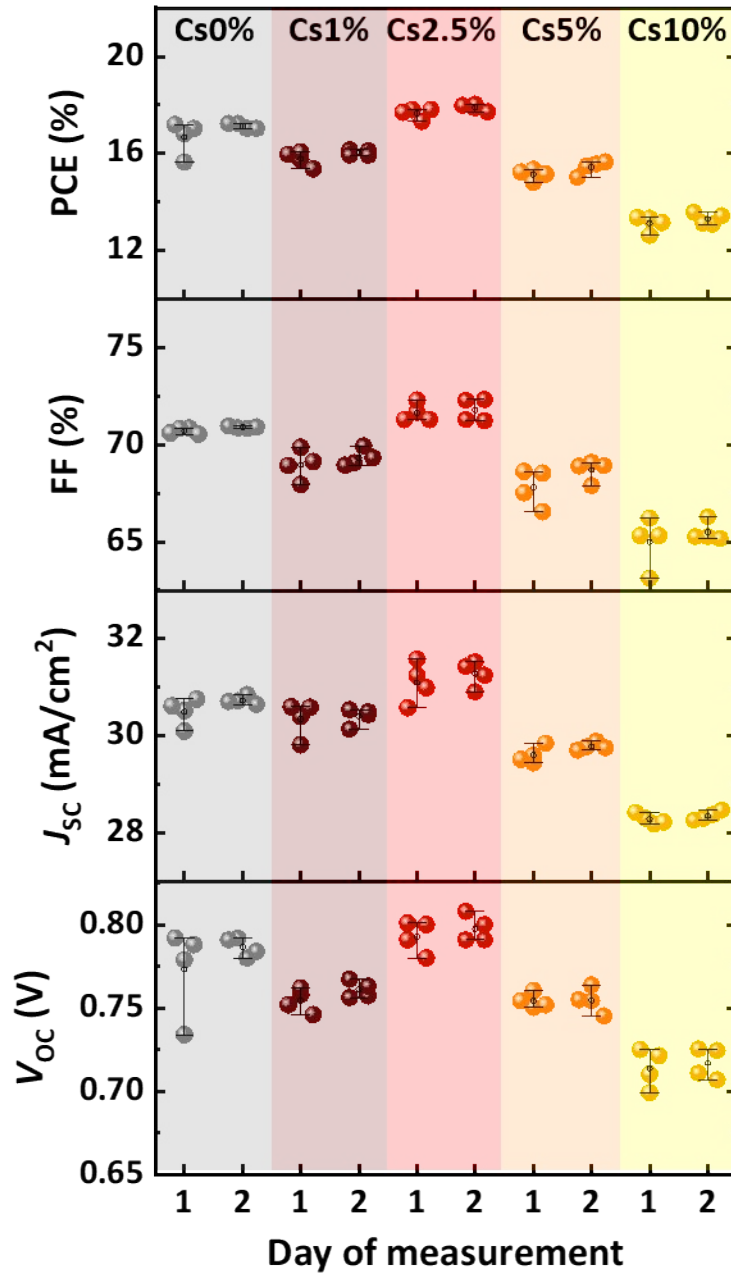


**Fig. S4.** Power conversion efficiency (PCE), fill factor (FF), short-circuit current ( $J_{sc}$ ), and open-circuit voltage ( $V_{oc}$ ) of champion PSCs (from different batches) with different Cs concentrations measured on day 1 (day of device completion) and day 2 (after one night of storage in a dark inert atmosphere).

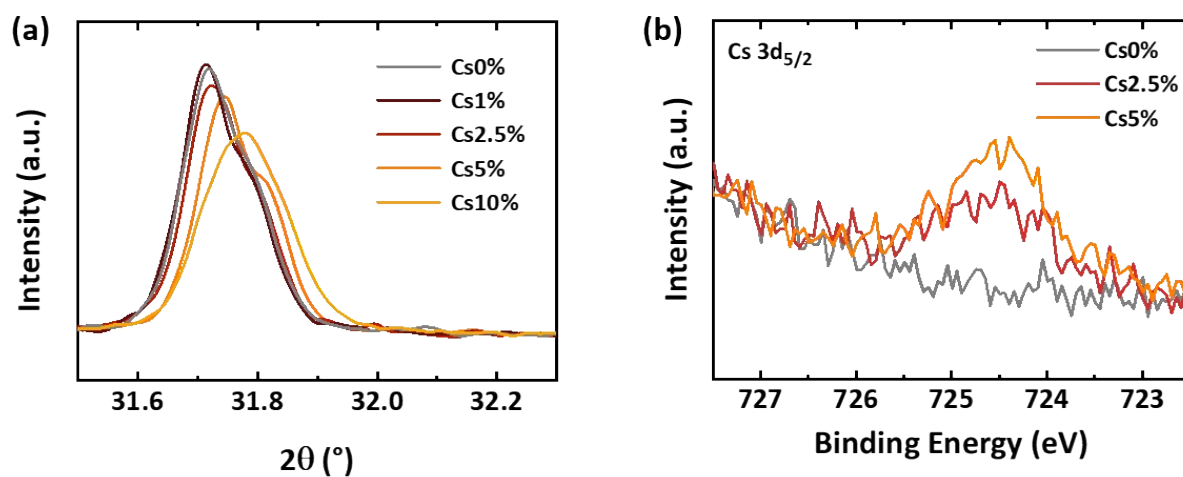


**Fig. S5.** (a) X-ray diffraction (XRD) peaks assigned to (114)/(310) planes of the  $\text{Cs}_x(\text{FA}_{0.8}\text{MA}_{0.2})_{(1-x)}\text{Sn}_{0.5}\text{Pb}_{0.5}\text{I}_3$  low-bandgap perovskite thin-films shifting to higher diffraction angles by increasing  $x$ . (b) X-ray photoelectron spectroscopy (XPS) spectra of the Cs  $3d_{5/2}$  core level of the low-bandgap perovskite thin-films samples with different Cs concentrations varying from 0% to 2.5% and 5%.

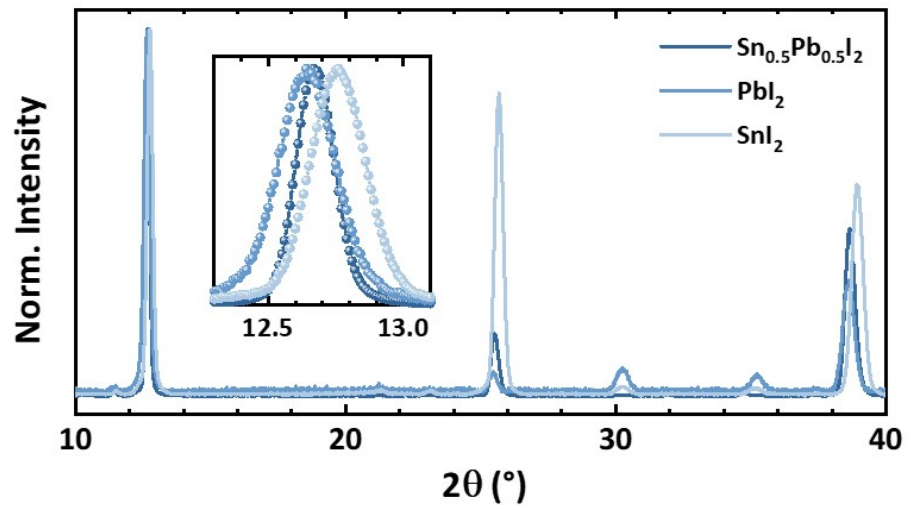


**Fig. S6.** XRD patterns collected from  $\text{PbI}_2$ ,  $\text{SnI}_2$ , and  $\text{Sn}_{0.5}\text{Pb}_{0.5}\text{I}_2$  thin-films (inset compares the position of the main peak of the three thin-films).



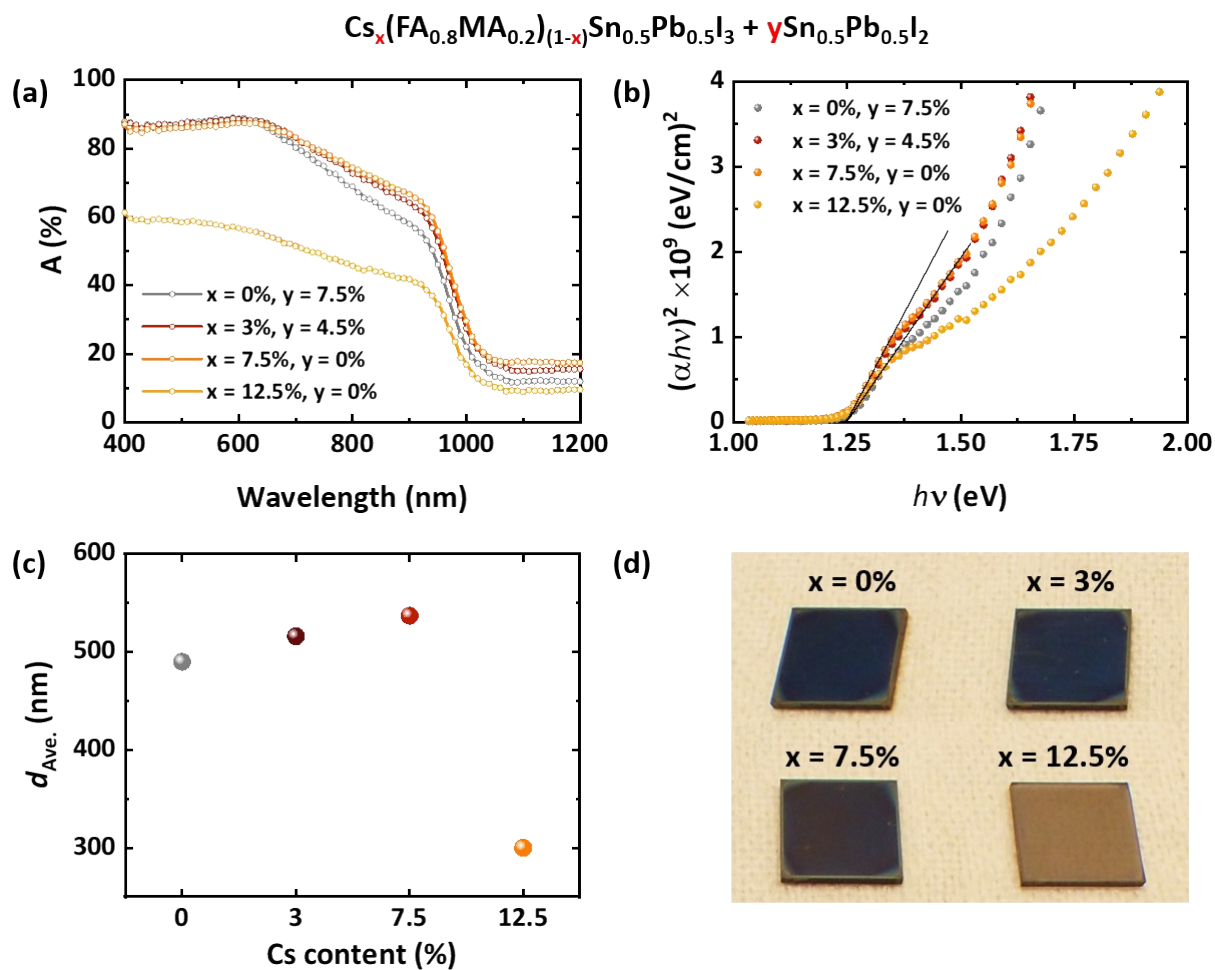


**Fig. S7.** (a) Absorbance spectra (A), (b) Tauc plot, (c) the average thickness ( $d_{\text{Ave.}}$ ), and (d) picture of  $\text{Cs}_x(\text{FA}_{0.8}\text{MA}_{0.2})_{(1-x)}\text{Sn}_{0.5}\text{Pb}_{0.5}\text{I}_3$  thin-films prepared with excess Sn and Pb for different Cs concentrations of  $x = 0\%$ ,  $3\%$ ,  $7.5\%$ , and  $12.5\%$ . All the thin-films are deposited on glass substrates. The average thickness ( $d_{\text{Ave.}}$ ) of each thin-film is an average of ten values obtained from two different samples on five different spots on each.

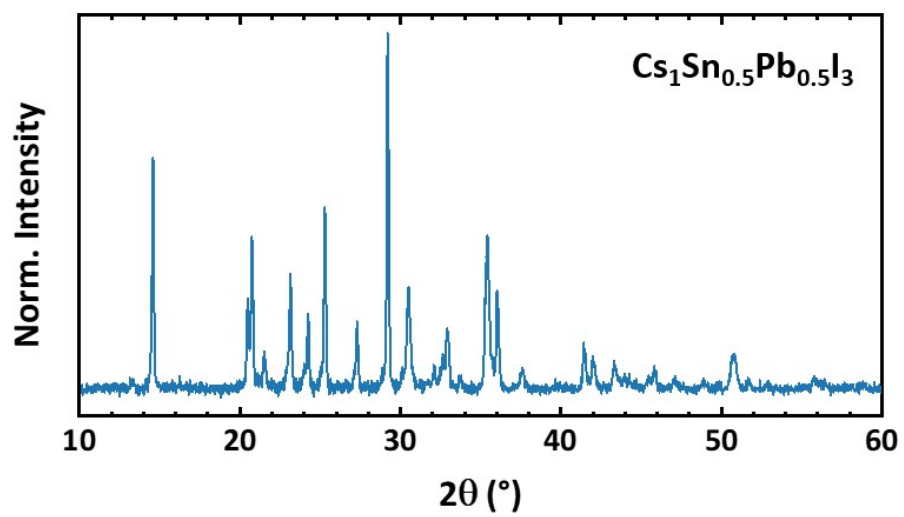


**Fig. S8.** X-ray diffraction (XRD) patterns of  $\text{Cs}_1\text{Sn}_{0.5}\text{Pb}_{0.5}\text{I}_3$  perovskite thin-film.

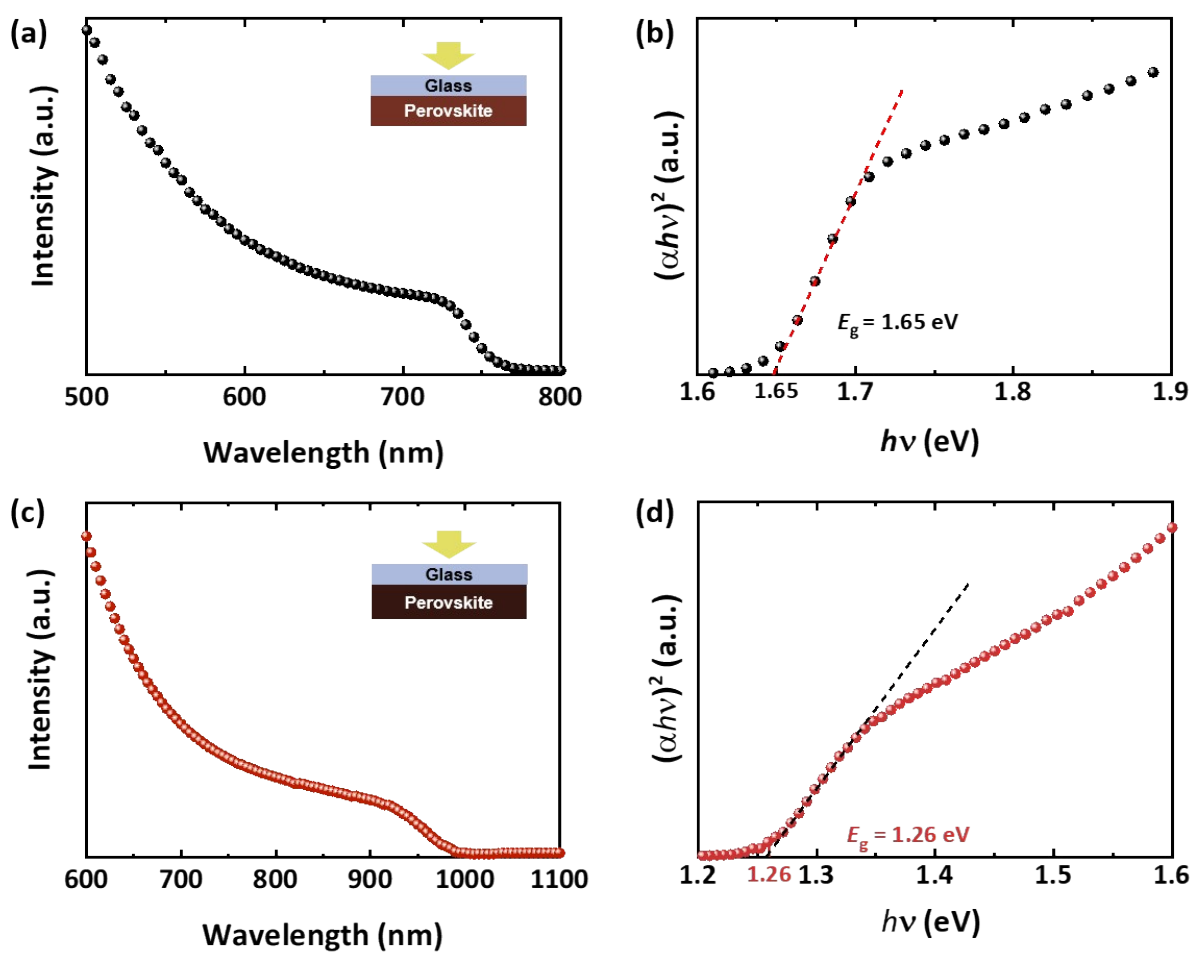
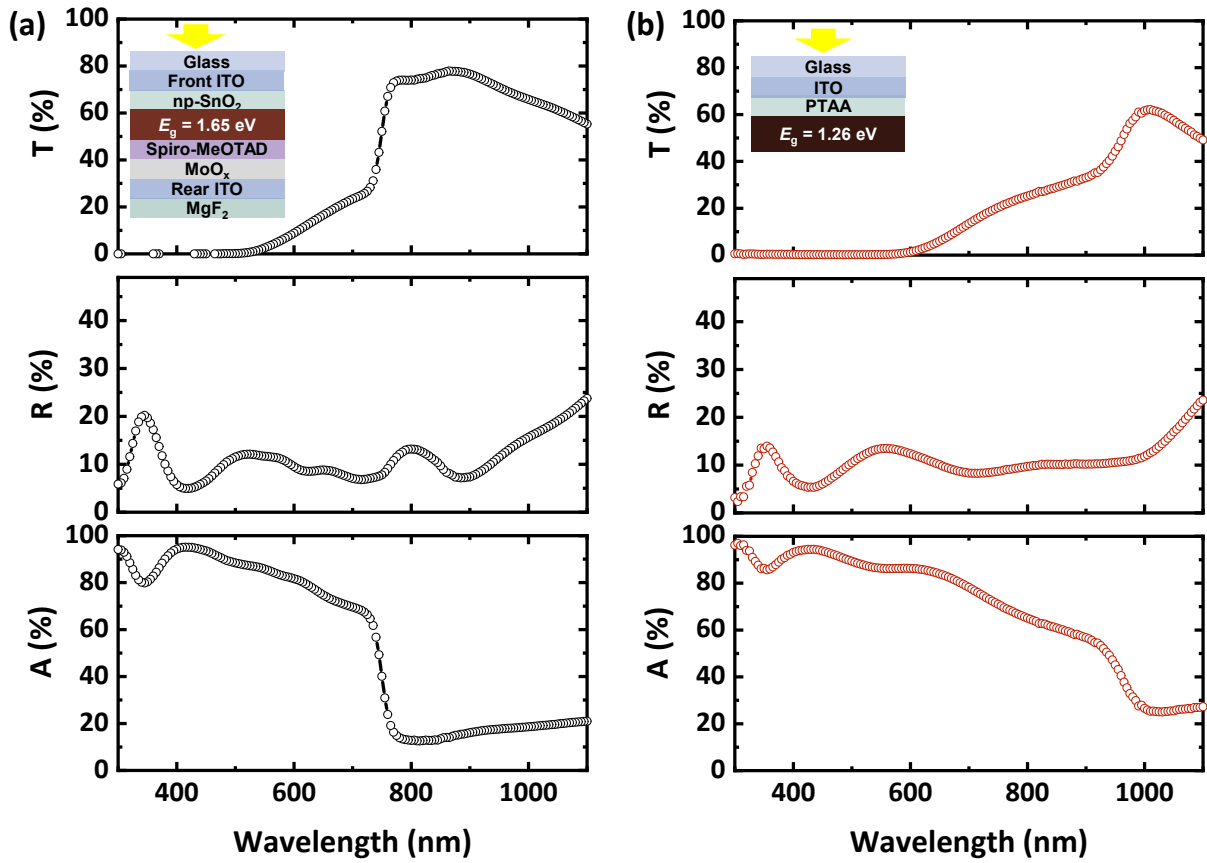
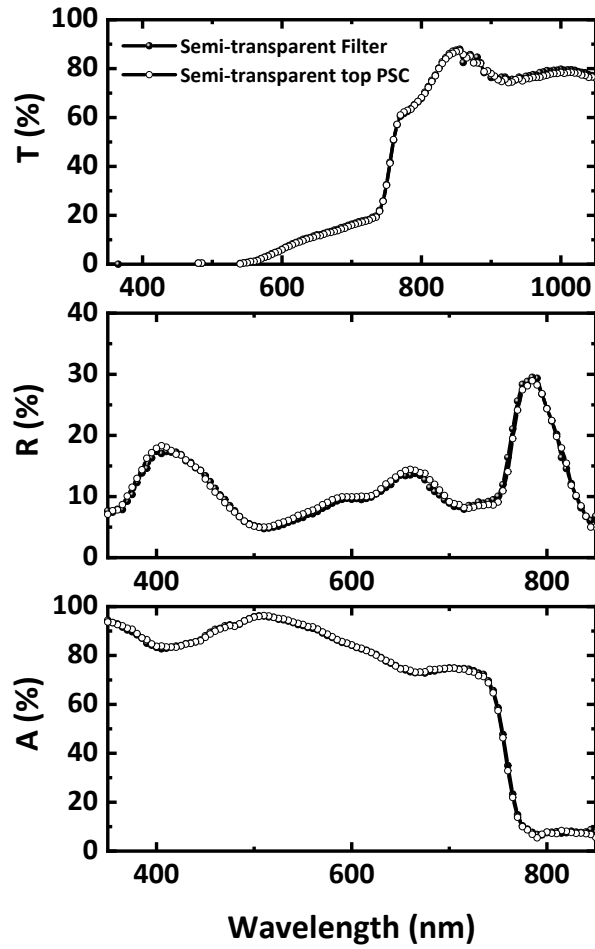


Fig.

S9. UV-vis absorbance spectra and Tauc plots of a double-cation  $\text{Cs}_{0.17}\text{FA}_{0.83}\text{Pb}(\text{I}_{0.76}\text{Br}_{0.24})_3$  perovskite thin-film with a bandgap of  $E_g = 1.65$  eV (a and b), and a triple cation  $\text{Cs}_{0.025}(\text{FA}_{0.8}\text{MA}_{0.2})_{0.075}\text{Sn}_{0.5}\text{Pb}_{0.5}\text{I}_3$  low-bandgap perovskite thin-film with a bandgap of  $E_g = 1.26$  eV (c and d), both deposited on glass substrates.



**Fig. S10.** Transmittance (T), reflectance (R), and absorbance (A) spectra of (a) a semitransparent perovskite filter composed of a double-cation  $\text{Cs}_{0.17}\text{FA}_{0.83}\text{Pb}(\text{I}_{0.76}\text{Br}_{0.24})_3$  perovskite thin-film with a bandgap of  $E_g = 1.65$  eV, and (b) a triple cation  $\text{Cs}_{0.025}(\text{FA}_{0.8}\text{MA}_{0.2})_{0.075}\text{Sn}_{0.5}\text{Pb}_{0.5}\text{I}_3$  low-bandgap perovskite thin-film with a bandgap of  $E_g = 1.26$  eV, deposited on PTAA-coated ITO.



**Fig. S11.** Transmittance (T), reflectance (R), and absorptance (A) spectra of a semitransparent perovskite filter and a semi-transparent top PSC, composed of a double-cation  $\text{Cs}_{0.17}\text{FA}_{0.83}\text{Pb}(\text{I}_{0.76}\text{Br}_{0.24})_3$  perovskite thin-film with a bandgap of  $E_g = 1.65$  eV. The relative difference in transmittance and reflectance on average (derived from three filters and three PSCs) is equal to  $\pm 1.1\%$  and  $\pm 0.1\%$ , respectively (weighted to AM1.5G).

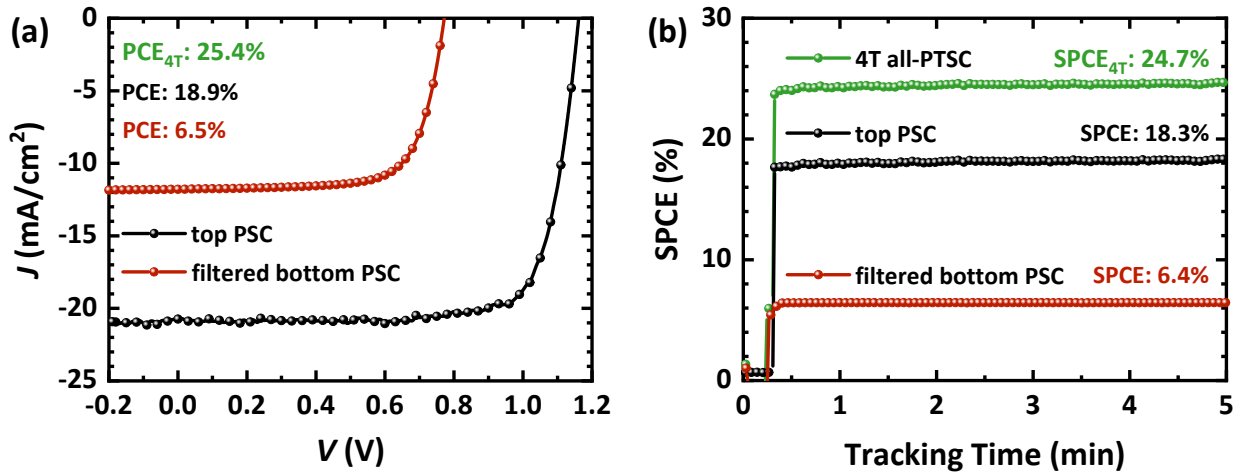


**Fig. S12.** (a) Current-density–voltage ( $J$ – $V$ ) scans measured at a fixed rate of 0.6 V/s from the open-circuit voltage ( $V_{OC}$ ) to the short-circuit current ( $J_{SC}$ ), and (b) maximum power point (MPP) tracking measurements of a single-junction semi-transparent top PSC ( $E_g = 1.65$  eV), a single-junction filtered LBG bottom PSC ( $E_g = 1.26$  eV) covered with an anti-reflection PDMS foil, under AM 1.5G illumination ( $100$  mW/cm<sup>2</sup>) at 25°C.  $PCE_{4T}$  and  $SPCE_{4T}$  are the calculated PCE and stabilized PCE derived from the  $J$ – $V$  scans and MPP tracking measurements for the champion 4T all-PTSC, respectively.

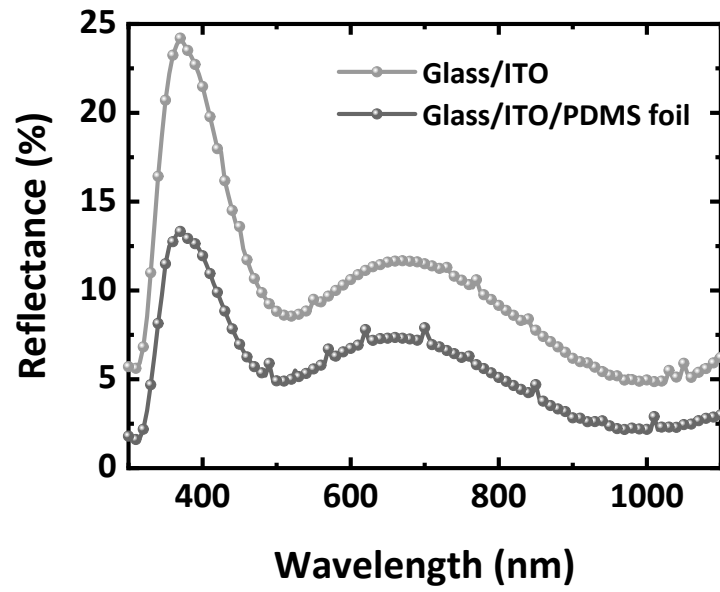


**Fig. S13.** Reflectance spectra of an ITO glass substrate with and without a textured PDMS foil implemented on the front-side of the ITO glass substrate.

**Table S2.** Photovoltaic parameters derived from current-density–voltage ( $J$ – $V$ ) scans measured at a fixed rate of 0.6 V/s from the open-circuit voltage ( $V_{OC}$ ) to the short-circuit current ( $J_{SC}$ ) (backward scan) and from  $J_{SC}$  to  $V_{OC}$  (forward scan) for a champion semi-transparent top PSC and a filtered LBG bottom PSC while an anti-reflection PDMS foil was applied in front side of the device. The stabilized PCEs (SPCEs) of the top and filtered bottom PSCs and the corresponding calculated 4T all-perovskite tandem solar cell (all-PTSC) are given in bold.

Perovskite solar cell (PSC)	Scan Direction	$V_{OC}$ (V)	$J_{SC}$ (mA/cm <sup>2</sup> )	FF (%)	PCE (%)	SPCE (%)
Semi-transparent top PSC (with PDMS)	Backward	1.16	20.7	78.6	<b>18.9</b>	<b>18.3</b>
	Forward	1.13	21.0	74.4	<b>17.7</b>	
Filtered LBG bottom PSC (with PDMS)	Backward	0.77	11.7	72.0	<b>6.5</b>	<b>6.4</b>
	Forward	0.76	11.7	67.5	<b>6.0</b>	
4T all-PTSC (with PDMS)	Backward				<b>25.4</b>	<b>24.7</b>
	Forward				<b>23.7</b>	